THE EFFECT OF ALIGNED MATRIX MATERIAL ON THE MECHANICS OF CRACKED FIBERS

E. L. Stanton

Prototype Development Associates, Inc.
Santa Ana, California 92705

Introduction

The present study examines computationally a crack problem with finite geometry and two orthotropic phases intended to represent a cracked graphite fiber surrounded by an aligned matrix phase or sheath. The scope of the study is strictly heuristic and is not intended as a replica modeling of any particular fiber-matrix system although representative elastic constants are used. Recent studies of an isotropic finite dimensional bar with a penny shaped crack [1] are used as a control problem to verify the computational model.

The Model

The control problem was modeled using symmetry with two isoparametric finite elements, Figure 1, with their parametrization adjusted to give singular strains in any direction emanating from the edge of the crack. This model produced good agreement with the earlier results of Gykenyesi and Mendelson for crack opening displacements and stresses in the neighborhood of the crack. The same geometric model was used for the fiber-matrix problem with properties as follows:

$E_T = 2$ msi , $E_L = 57$ msi (Fiber)

$E_T = 2$ msi , $E_L = 80$ msi (Aligned matrix)

$G_T = 0.5$ msi , $G_{TL} = 1$ msi (Both)

$\nu_T = 0$, $\nu_{TL} = 0.05$ (Both)

Note that high E/G ratios tend to reduce the accuracy of a model but should not change the character of the solution. Several boundary conditions were analyzed that produce uniform stress, uniform strain and uniform displacement respectively in the axial direction. The uniform strain condition was simulated by applying a uniform axial stress to each phase in proportion to its axial stiffness and is most representative of conditions in a long fiber. In all cases the total force applied to the model was constant and equal to that in the control problem. The high axial modulus of the aligned matrix simulates conditions thought to occur during processing. Note that this alignment of the basal planes is opposite to that of the sheath phase associated with densification by chemical vapor deposition (CVD).

Results

The crack opening displacements shown in Figure 2 for the isotropic case have nearly damped out at the loaded surface. Significantly larger crack opening displacements occur in the graphite fiber for both uniform stress and uniform strain boundary conditions as a result of the low shear modulus. They are respectively 1.25E-4, 2.50E-4, and 1.77E-4 inches for the isotropic uniform stress, orthotropic uniform stress and orthotropic uniform strain conditions. The appearance of the deformations in the uniform strain case is nearly identical to that in Figure 2 when normalized to the same scale. However, the uniform stress case resulted in clearly visible axial displacements at the loaded surface when displayed to the same scale. The uniform displacement boundary conditions produced an unusual result that may be more a mathematical curiosity than fiber-matrix mechanics. In this case the center of the crack surface displaced very little producing a shape like the beam function associated with a unit rotation at the edge of the crack.

The axial stress in the plane of the crack as a function of the parametric coordinate, $\xi = \sqrt{r/0.77}$, is shown in Figure 3 for the control problem and the orthotropic uniform strain case. Stresses proportional to the square root of the radius appear as linear functions of this coordinate. The finite element stresses are recovered at the Gaussian points and extrapolated to the boundary which accounts for their finite amplitude. Note that the axial stress in the orthotropic matrix material is higher and a more nonlinear function of the parametric coordinate indicating the strength of the singularity has increased. This one parameter, however, does not adequately describe the mechanics of the cracked fiber-matrix system. A contour plot of the ϵ_{13} shear strain over the Z_1 , Z_3 face of the two element model, Figure 4, shows this strain propagates strongly all along the fiber-matrix interface. As a result of this behavior, the crack would be more likely to result in disbonding of the two phases than fracture of the matrix phase in the plane of the crack. The driving force for this behavior can be explained in terms of the equilibrium equations

$$\begin{aligned} \sigma_{11,1} + \sigma_{12,2} + \sigma_{13,3} &= 0 \\ \sigma_{31,1} + \sigma_{32,2} + \sigma_{33,3} &= 0 \end{aligned} \qquad (1)$$

in which the terms $\sigma_{12,2}$ and $\sigma_{32,2}$ are zero by virtue of axial symmetry. The sharp gradient in the radial stress in the radial direction, $\sigma_{11,1}$ is accentuated by the bimaterial interface as is evident from the ϵ_{11} strain contours shown in Figure 5. It is also evident from these contours that greater modeling detail would be required to obtain high resolution of the stress response. Nevertheless these figures provide an insight into the mechanics of the problem comparable to photoelastic analyses.

Conclusions

The results presented indicate that a cracked fiber with an aligned matrix phase is likely to disbond at the fiber-matrix interface under uniform axial strain conditions. Computational mechanics in this case provided an insight into material behavior comparable to photoelastic studies in isotropic models. This is a particularly useful approach in the study of load redistribution in highly anisotropic carbon composites damaged during processing.

References

1. Gyekenyesi, J. P. and Mendelson, A., "Three-Dimensional Elastic Stress and Displacement Analysis of Finite Geometry Solids Containing Cracks," NASA TM-X-71467, 1974.

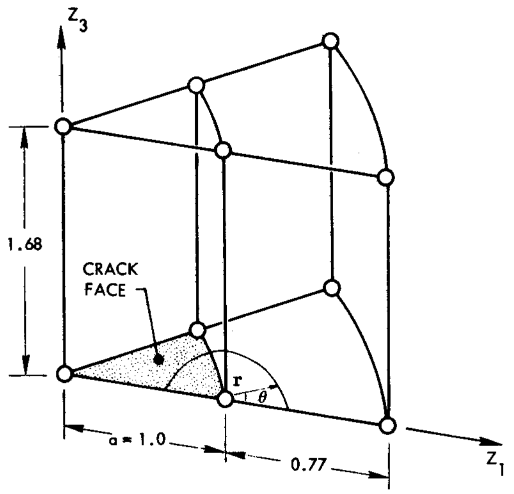

Figure 1. PATCHES-III model of cracked fiber

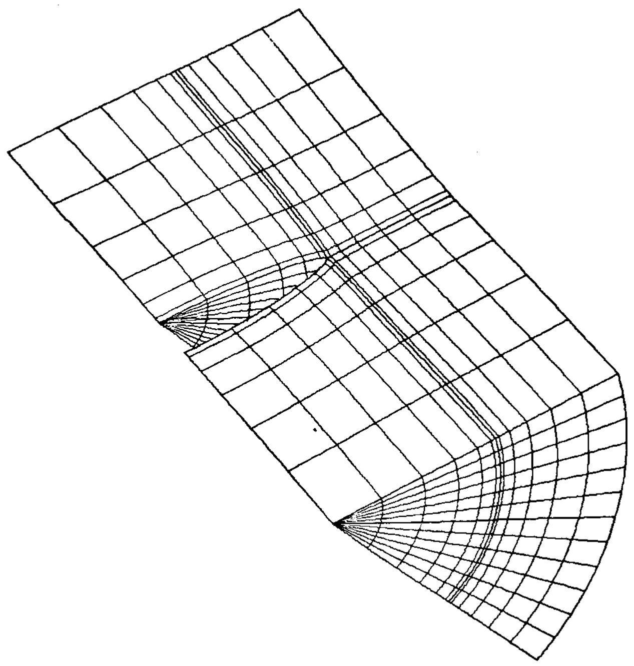

Figure 2. Cracked fiber elastic deformations

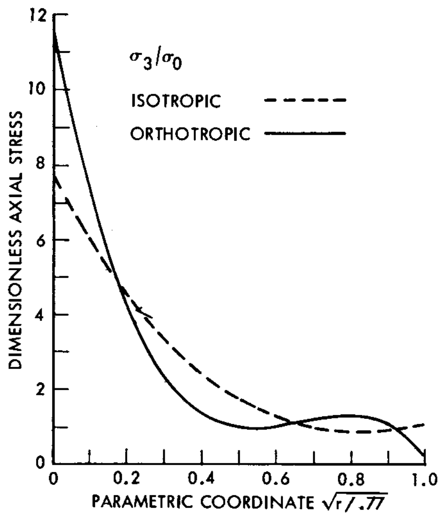

Figure 3. Axial stress comparisons

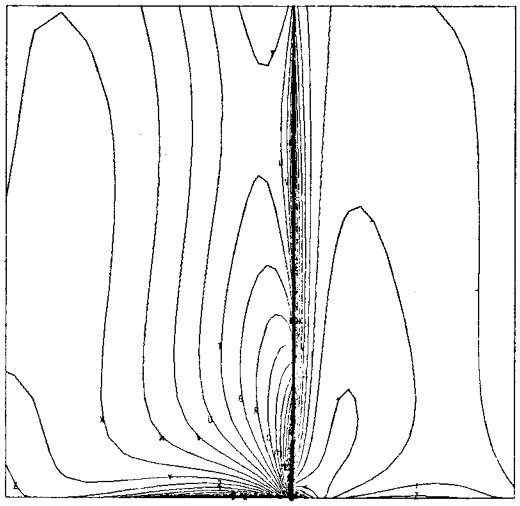

Figure 4. Shear strain contours ϵ_{13}

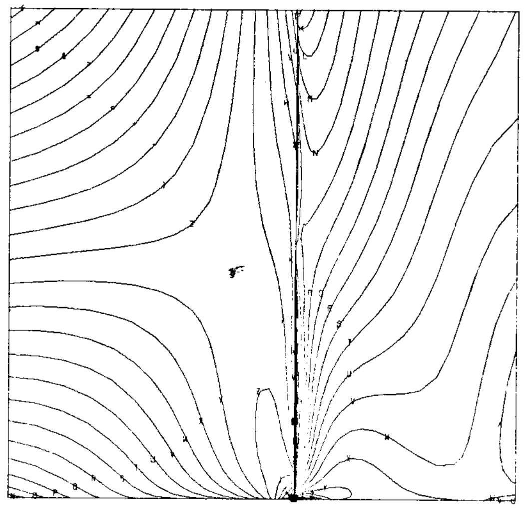

Figure 5. Radial strain contours ϵ_{11}